Article

Experimental Study on Energy Dissipation Performance of SPA Shear Plate Metal Damper Based on Jacket Platform

Jiakang Li [1], Zhe Zhang [1,*], Lu Wang [1], Zhe Ma [2] and Wenyuan Wang [2]

1   School of Civil Engineering, Nantong Institute of Technology, Nantong 226000, China;
    jiakang_li@163.com (J.L.); wanglu010872@163.com (L.W.)
2   Faculty of Infrastructure Engineering, Dalian University of Technology, Dalian 116024, China;
    deep_mzh@dlut.edu.cn (Z.M.); wangwenyuan@dlut.edu.cn (W.W.)
*   Correspondence: 20239078@ntit.edu.cn

Abstract: Aiming at the problem of excessive vertical vibration caused by seismic primary waves in jacket structures located in seismic zones in China, a new type of shear plate metal damper with upper and lower elliptical openings (SPA) is proposed in this paper. The seismic model test is carried out to compare the shear plate metal damper with three traditional opening forms, central elliptical opening, single row opening, and double row opening, and the hysteretic curve, skeleton curve, and cyclic hysteretic energy dissipation capacity are analyzed. The results show that the energy dissipation performance of the new shear plate metal damper with upper and lower elliptical openings proposed in this paper is better than that of the other three types of dampers.

Keywords: jacket foundation; seismic load; shear plate metal damper; hysteretic energy dissipation

1. Introduction

The development of marine engineering is very important for the development and utilization of marine resources [1,2]. At present, China's marine development of shoals and offshore areas has continued to increase, and jacket foundations have been widely used, due to their advantages such as a simple structure, safety and reliability, low cost, and little influence by waves and current loads [3–6]. The Bohai Sea, the Yellow Sea, and the southeast coast of China are earthquake-prone areas [7,8]. In addition to typical wind, waves, and current loads, offshore marine engineering construction in China also faces the potential threat of seismic loads [9].

A seabed earthquake has strong uncertainty and randomness. The seismic action will affect the mechanical behavior of each component of the offshore platform itself and between the components, resulting in a change in the vibration response of the platform structure. A seismic primary wave will affect the vertical vibration response of the structure. The jacket platform has dynamic sensitivity, and it is prone to excessive multi-modal vibration under complex seismic loads, which greatly affects the daily operation of offshore platforms and may cause structural fatigue damage [10–12]. In order to ensure the safe and reliable operation of an offshore platform, it is necessary to control the vibration of the offshore platform under load to prolong the service life of the platform and reduce the maintenance cost of the platform [13]. Passive energy dissipation technology has been widely used in the field of marine engineering due to its economy, effectiveness, reliability, and easy implementation [14,15].

Ke et al. [16] studied the effectiveness of a shape memory alloy and wedge friction plate self-centering damper (SMA-VFSD), with multiple energy dissipation mechanisms, in improving the seismic performance of structures under seismic loads. The results show that the multiple energy dissipation mechanisms of SMA-VFSDs are beneficial in reducing the inelastic seismic response of structures. Zuo et al. [17] applied multiple-tuned mass dampers (MTMD) to a fixed offshore platform structure and studied the control effect

of the MTMD on structural vibrations under an earthquake by numerical simulation. Wang et al. [18] used the amplified damping transmission system (ADTS) to control the vibration of the jacket platform under an earthquake. The results show that compared with the traditional mass damper (TMD), ADTS has better performance in controlling seismic responses due to its higher additional damping. Zhang et al. [19] proposed a tuned mass damper (TMDI) to reduce the vibration of offshore platforms under wind–wave–earthquake combined loads. The results show that TMDI is superior to TMD in suppressing wind–wave–earthquake coupling response. The above energy dissipation structures are mainly used to suppress the horizontal vibration response of marine structures under earthquake action, while the vertical vibration response of marine structures should not be ignored.

At present, the shear plate metal damper is usually used to control the vertical vibration of the structure, and the opening form of the damper will directly affect the energy dissipation efficiency of the damper. The stress concentration of the shear plate metal damper in the traditional opening form is more severe, resulting in poor energy dissipation capacity. Based on this, this paper proposes a new type of shear plate metal damper, which is a shear plate metal damper with upper and lower elliptical openings. The new damper is arranged in the middle of the horizontal brace, as shown in Figure 1. It can first yield to dissipate energy under a seismic load, effectively reduce the vertical vibration response of the structure caused by the primary wave, and protect the safety of the whole structure. The new shear plate metal damper mainly uses the plastic deformation of structural components to dissipate seismic energy. It not only has superior energy dissipation performance [20,21] but also has the advantages of a simple structure, low cost, and easy replacement after damage [22]. It can effectively reduce the damage to the jacket platform caused by the seismic load and the maintenance cost of the platform after the earthquake.
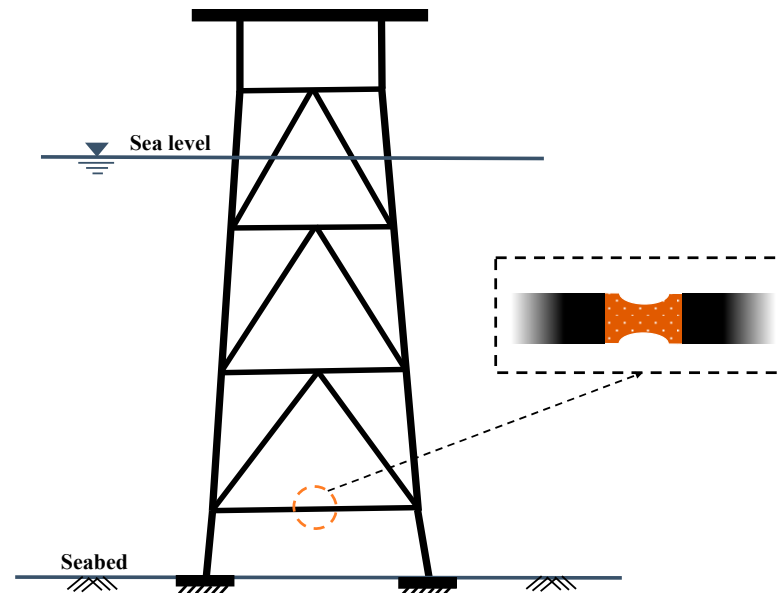

Figure 1. Installation position diagram of new shear plate damper [23].

In this paper, a new type of shear plate metal damper with upper and lower elliptical openings suitable for jacket platforms is proposed and compared with the other three traditional opening forms (central elliptical opening, single row opening, and double row opening). The energy dissipation performance of the new shear plate metal damper is explored by loading test. The section of this paper is divided into the following four parts: Section 2 shows the experimental basis; Section 3 comprises the performance study of the new damper; Section 4 presents the conclusion and future of this paper.

2. Test Basis

2.1. Shear-Type Steel Plate Damper Selection

(1)   Entire plate without opening form

Because the damper is sheared as a whole, the bending movement at both ends is the largest, so the stress at both ends of the shear plate is the largest, and stress concentration can occur easily, resulting in premature failure of the damper.

(2)   Centralized opening form

Centralized opening refers to the form in which the openings are concentrated and the position edges are closed. This form is widely used in dampers with steel as the matrix. The opening position is usually the shear web, the opening is generally an approximate diamond, and the diamond is circularly transitioned to avoid stress concentration. The diamond opening is to enable the web to yield most of the energy consumption and enhance the energy dissipation capacity of the damper. The reasonable yield order is that the weakest section yields first, and the strength of the material is hardened to achieve the purpose of yielding most of the web. Such dampers are generally designed as shear-yielding energy dissipation components. Even so, the failure of most metal dampers in the form of central diamond openings is also due to an improper opening size or angle, resulting in cracking failure at the diamond corner position on the web.

(3)   Distributed opening form

Distributed opening refers to the dispersed opening form located inside or at the edge of the damper. This kind of damper is combined with each others in terms of the number of openings, the style of openings, the location of openings, and the various configurations of the damper matrix, which can form a variety of distributed opening forms. The more common forms include single-row openings and multi-row openings. A distributed opening damper has better energy dissipation capacity and more uniform plastic distribution. In recent years, scholars at home and abroad have done considerable research on the above two forms of shear plate dampers and put forward a large number of open-hole configurations.

In summary, this paper proposes a shear plate damper configuration in the form of upper and lower elliptical openings. This form also belongs to the distributed opening form. The elliptical opening avoids the generation of stress concentration to the greatest extent. At the same time, it has the advantages of simple configuration and convenient industrial processing.

2.2. Shear Steel Damper with Different Opening Forms

The four forms of shear plate damper configurations are introduced as follows. The specific design parameters are shown in Table 1:

(1)   The form of upper and lower elliptical openings: the shear plate is open with a semi-elliptical hole, and the ratio of the long axis to the short axis is 2:1, which is recorded as SPA (Shear Plate A), as shown in Figure 2a.

(2)   The form of the central elliptical hole: the central elliptical hole of the shear plate is recorded as SPB (Shear Plate B), as shown in Figure 2b.

(3)   Single-row opening form: the shear plate has dispersed single-row openings, and the end of the hole groove is designed as a circle, which is recorded as SPC (Shear Plate C), as shown in Figure 2c.

(4)   Double-row opening form: The shear plate has dispersed double-row openings, and the end of the hole groove is designed as a circle, which is recorded as SPD (Shear Plate D), as shown in Figure 2d.

Table 1. Design parameters of shear plate damper openings.

Type	Opening Rate	A (mm)	B (mm)	C (mm)	D (mm)
SPA10	10%	106.84	26.71	--	--
SPA15	15%	130.84	32.71	--	--
SPA20	20%	151.08	37.77	--	--
SPA25	25%	128.92	42.23	--	--
SPB10	10%	106.84	53.42	--	--
SPB15	15%	130.84	65.42	--	--
SPB20	20%	151.08	75.54	--	--
SPB25	25%	168.92	64.46	--	--
SPC10	10%	74.67	16.98	27.26	--
SPC15	15%	91.45	20.78	24.42	--
SPC20	20%	105.6	24.00	22.00	--
SPC25	25%	118.06	26.84	19.87	--
SPD10	10%	30.68	16.98	27.27	60.00
SPD15	15%	37.57	20.77	24.42	60.00
SPD20	20%	43.38	24.00	22.00	60.00
SPD25	25%	48.50	26.84	19.87	60.00

(**a**) SPA

(**b**) SPB

(**c**) SPC

(**d**) SPD
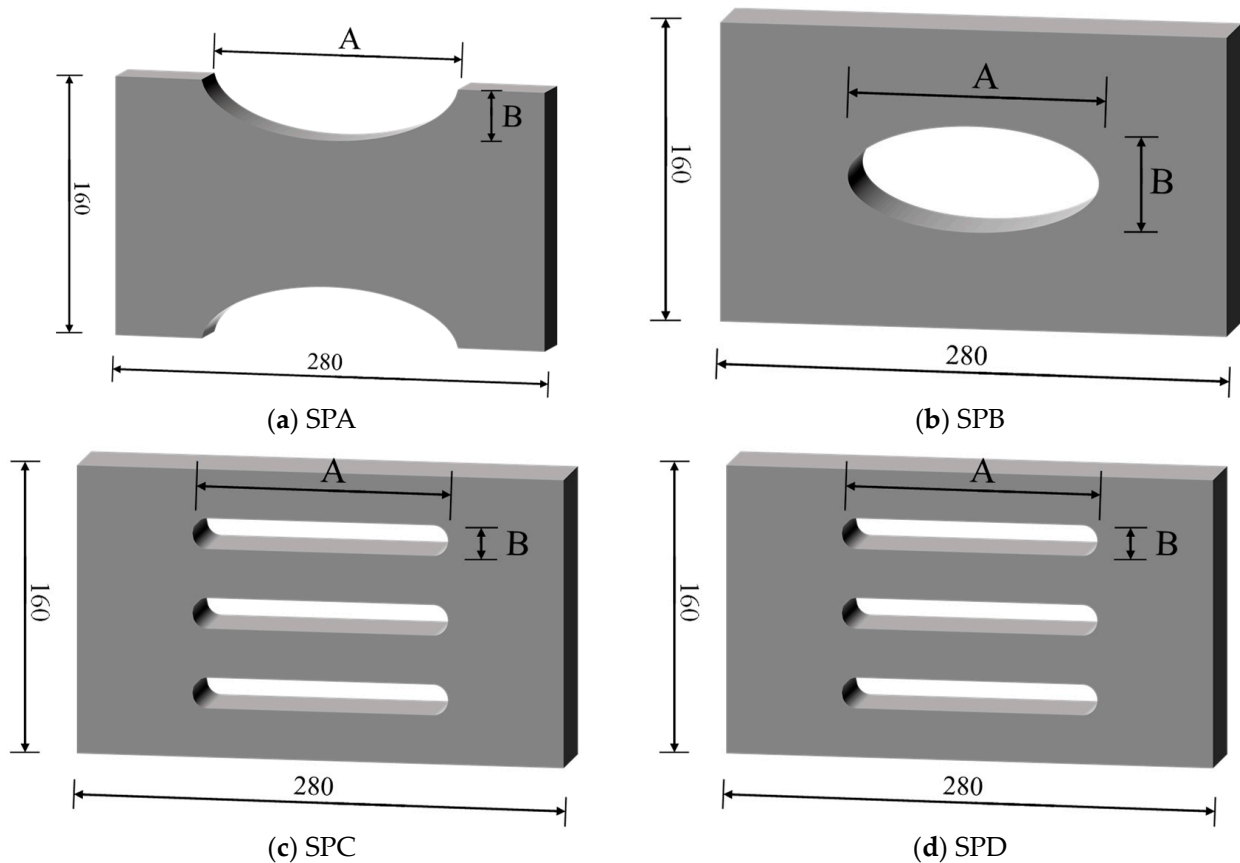
Figure 2. Design schematics of four kinds of shear plate dampers (mm).

2.3. Constitutive Relationship of Materials

The four kinds of damper materials are all Q235 steel, and their physical and mechanical properties are shown in Table 2, where ρ is the material density, E is the elastic modulus, μ is the Poisson's ratio, C is the specific heat capacity, σ_b is the ultimate strength, and σ_y is the yield strength. In order to obtain the actual yield strength of the material, the tensile test of the standard specimen of the same batch of steel was carried out. The material's constitutive relationship is shown in Figure 3, where σ is stress, and ε is strain.

Table 2. Physical and mechanical properties of Q235 steel.

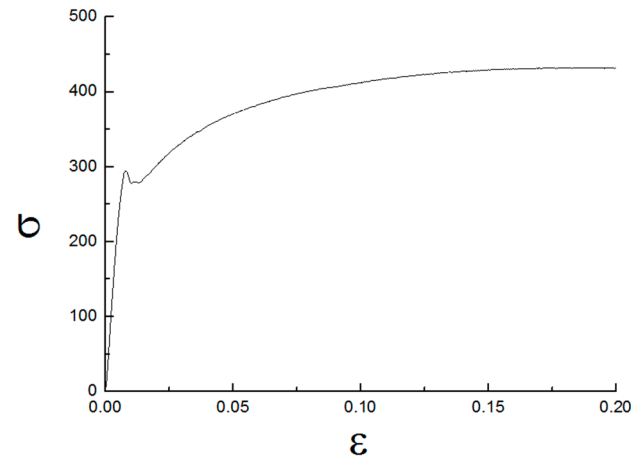| ρ (kgm^{-3})	E (MPa)	μ (−)	C (Jkg^{-1}K^{-1})	σ_b (MPa)	σ_y (MPa)
7860	2.07×10^5	0.3	504	406	235

Figure 3. Experimental curve of constitutive relation of component material.

2.4. Test Equipment

In this paper, the loading test of the specimen is carried out by using a 30 t MTS testing machine. The load range of the test machine is ±30 KN (large sensor) and ±1 KN (small sensor), the load accuracy is ±0.5%, the maximum displacement is 1000 mm, and the control mode is displacement and load. The fixture is a double-layer antisymmetric L-shaped bracket with a single-layer thickness of 20 mm. The yield strength of the material is about 235 MPa and the ultimate strength is 406 MPa. The two ends of the component are tightened with the fixture through 12 high-strength bolts. The double-layer fixture is connected by 20 high-strength bolts, and the component is held at the center of the fixture. The upper and lower ends of the fixture are welded with holding rods with a diameter of 36 mm, as shown in Figure 4.
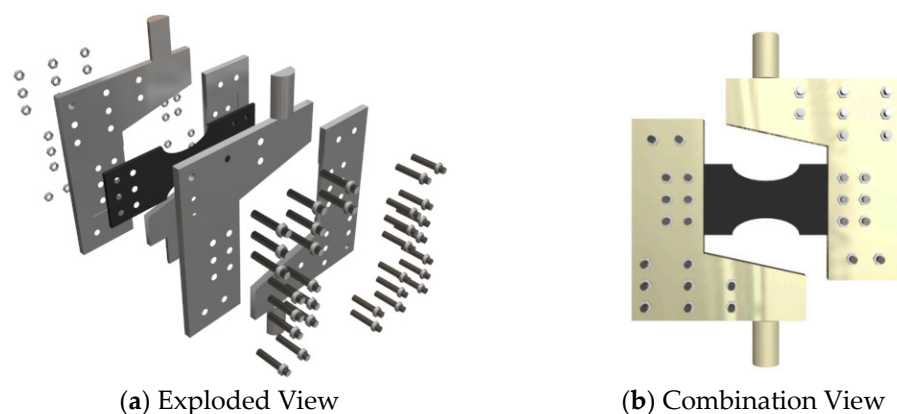

(**a**) Exploded View   (**b**) Combination View

Figure 4. Schematic diagram of experimental components.

The upper and lower ends of the loading frame are connected with the MTS testing machine, and the fixture transforms the tensile loading into the shear loading of the component, as shown in Figure 5a. The shear reciprocating loading test of the coupling beam damper is realized by the axial reciprocating loading test of the upper actuator of MTS.
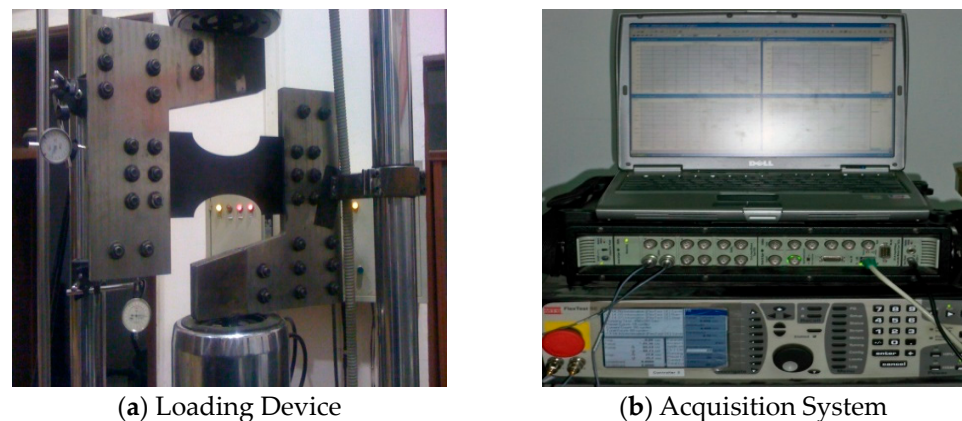
(**a**) Loading Device

(**b**) Acquisition System

Figure 5. Test loading device and acquisition system.

The loading frame has enough stiffness to satisfy the full transfer of the loading displacement to the damper end. During the experiment, two dial gauges were placed at the end of the loading frame to observe the horizontal displacement and vertical displacement of the loading frame, respectively. The results show that the displacement generated is very small and can be ignored relative to the loading displacement. The test data is collected by the test machine's own acquisition system, as shown in Figure 5b.

3. Study of the Performance of the New Damper

In this section, the hysteretic curves, skeleton curves, and energy dissipation performance indexes of the four kinds of shear plate metal dampers (SPA, SPB, SPC, and SPD) with different opening forms are calculated. The purpose is to explore the anti-vibration performance of the new shear plate metal damper (SPA), with upper and lower elliptical openings, under the action of seismic primary waves.

3.1. Damper Loading Deformation and Failure Modes

Taking the opening rate of 25% as an example, Figure 6 lists the loading deformation and failure modes of the four kinds of shear plate dampers with openings. The deformation diagram corresponds to the deformation of the shear plate when it reaches the peak shear force. It can be seen from Figure 6 that the overall yield phenomenon of the four types of shear plates is obvious. The form of deformation in Figure 6 shows that SPA, SPB, and SPD have a certain overall out-of-plane phenomenon, while SPC has a local out-of-plane phenomenon due to the small center stiffness, but the overall planeness is good.

(**a**) SPA Deformation

(**b**) SPA Destruction

Figure 6. *Cont.*

(**c**) SPB Deformation

(**d**) SPB Destruction

(**e**) SPC Deformation

(**f**) SPC Destruction

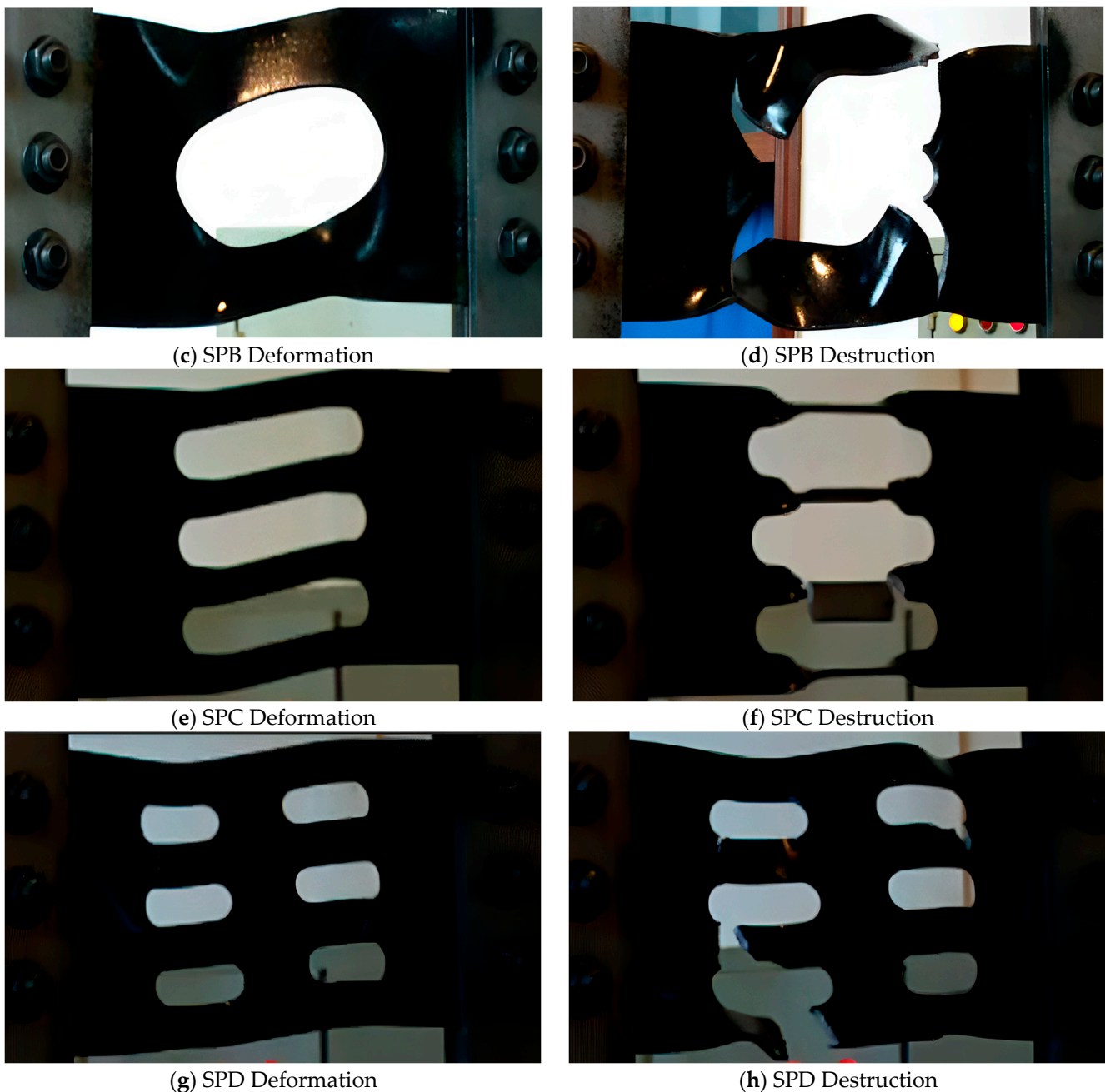(**g**) SPD Deformation

(**h**) SPD Destruction

Figure 6. Loading deformation and failure modes of different forms of shear plate dampers.

3.2. Load-Displacement Hysteretic Curve

In order to better compare the hysteresis performance of different forms of shear plate dampers, the abscissa of the hysteresis curve uses the shear displacement angle, and the ordinate uses the measured shear load. The hysteresis curves of the four types of shear plate dampers with four opening rates are obtained, as shown in Figures 7–10.

Figure 7 shows the hysteresis curve of the SPA series shear plate damper. It can be seen from the figure that the shape and change trend of the hysteresis curve under different opening rates are basically the same, and the secondary stiffness increases significantly after loading 1 mm displacement. The peak shear force of the damper decreases with the increase in the opening rate. The peak shear force of SPA10 is 74.22 KN, and the peak shear force of SPA15 is equivalent to it. The peak shear force of SPA20 and SPA25 decreased obviously, about 60 KN, which was 80% of the peak shear force of SPA10. At the same time, it can be seen that the bearing capacity of SPA series dampers after failure is between

30 KN and 40 KN, which decreases to about half of the peak shear force. From the point of view of the failure mode, the upper and lower sides of the central area of the shear plate are first torn along the inclined 45° direction, the central connection area provides some residual stiffness, and the bearing capacity before and after yield is quite different.
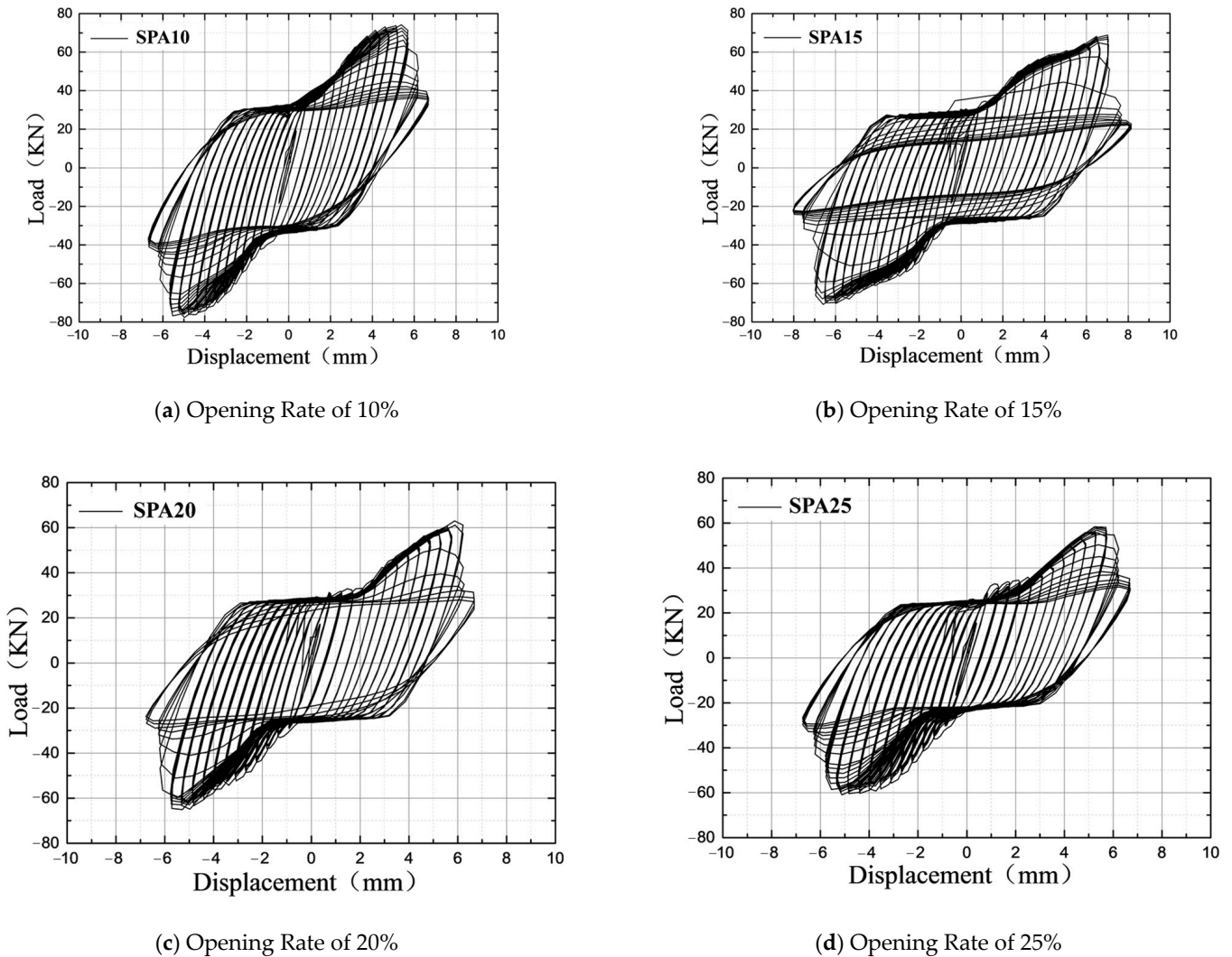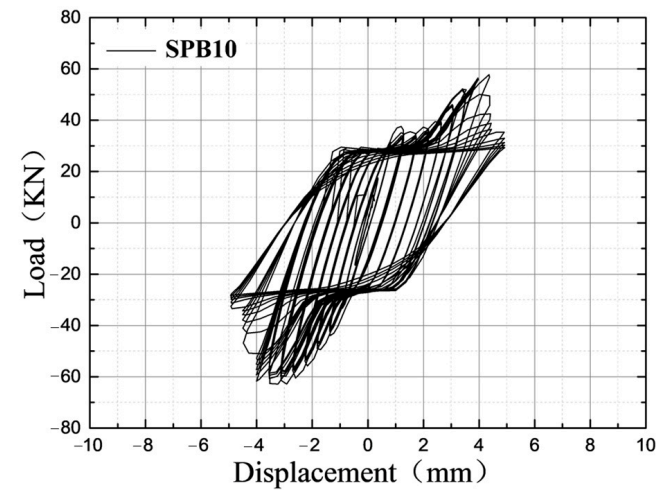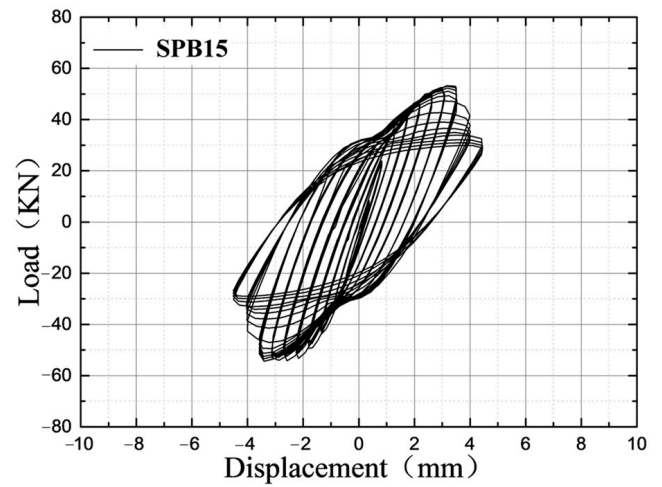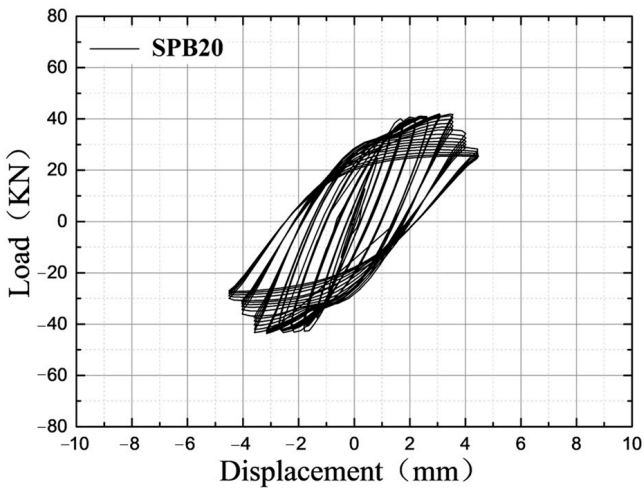

(**a**) Opening Rate of 10%

(**b**) Opening Rate of 15%

(**c**) Opening Rate of 20%

(**d**) Opening Rate of 25%

Figure 7. Hysteresis curve of SPA damper.

Figure 8 shows the hysteresis curve of the SPB series shear plate damper. It can be seen in the figure that the shape and change trend of the hysteresis curves of SPB15, SPB20, and SPB25 are basically the same, while the hysteresis curve of SPB10 after failure is fuller than that of the other three forms of opening rate. The peak shear force is 58.77 KN, which is basically the same as the peak shear force of SPB15. The peak shear force of SPB25 is 33.86 KN, which is about 58% of the peak shear force of SPB10. The bearing capacity of the SPB series dampers after failure is between 20 KN and 30 KN. From the perspective of the failure mode, the central area of the shear plate (corresponding to the same area as SPA) is torn up and down along the inclined 45° direction. After short-term stiffness strengthening, the structure fails, and the bearing capacity before and after yield is also quite different.
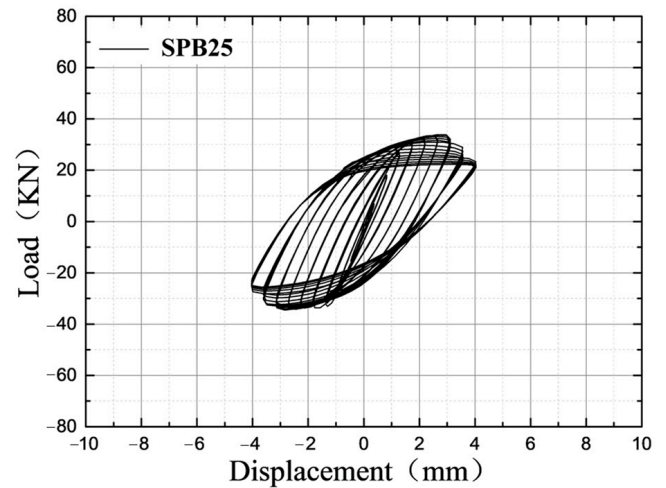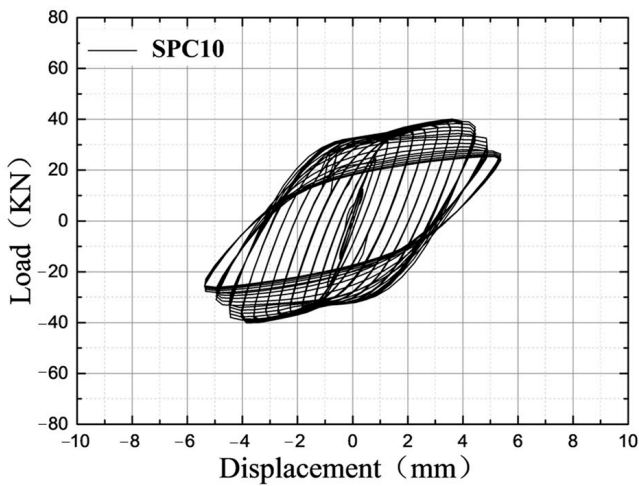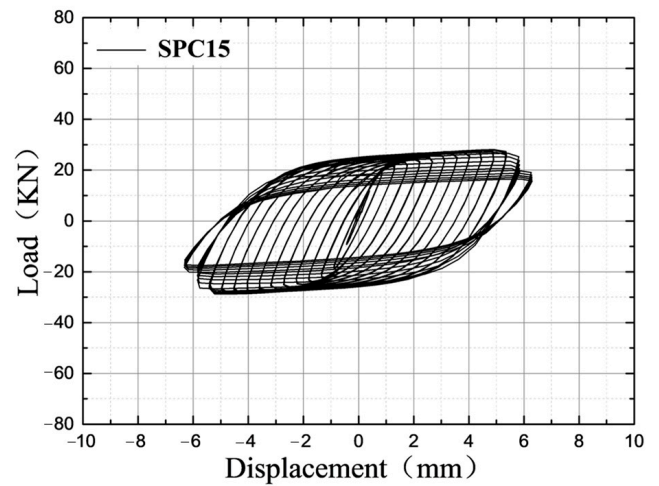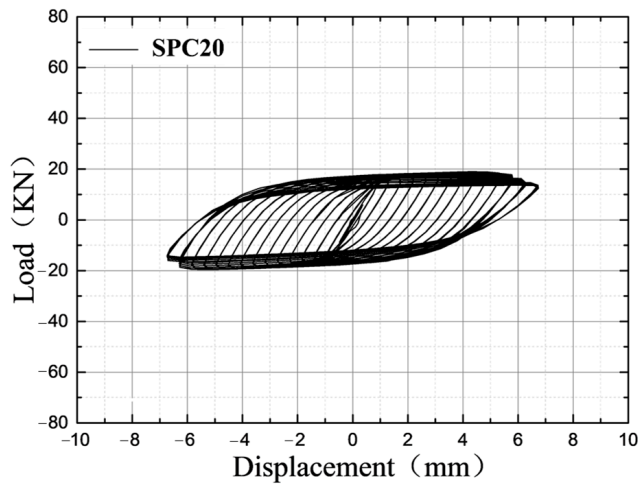
Figure 8. Hysteresis curve of SPB damper.

Figure 9 shows the hysteresis curve of the SPC series shear plate damper. In Figure 9, it can be seen that the hysteresis curve shape of the SPC damper is very full, but the peak shear force is relatively small. Moreover, the larger the opening rate of the damper, the less obvious the secondary stiffness enhancement. At the same time, it can be seen that the difference in the bearing capacity of the SPC series damper with four opening rates after failure is larger than that of the SPA and SPB series, between 15 KN and 40 KN. This is due to the small shear stiffness in the middle of the single-row hole shear plate, which leads to the secondary strengthening that is not obvious. Although it enters the failure state very early, it can be continuously loaded to 9 mm. After the failure, the central line is turned over, and finally, the tear is destroyed and separated from the matrix.
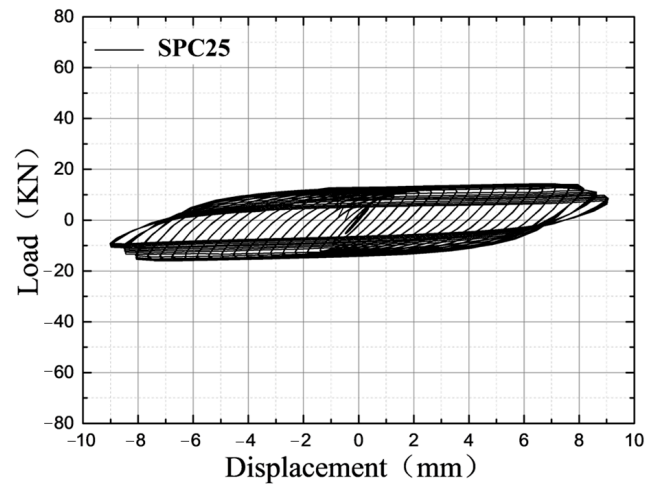
(**a**) Opening Rate of 10%

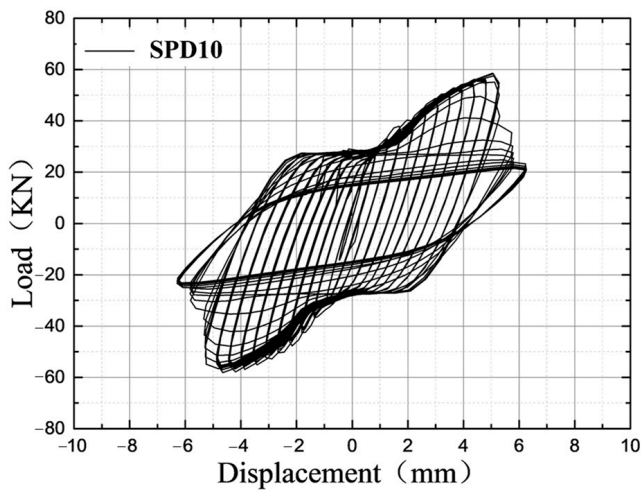(**b**) Opening Rate of 15%

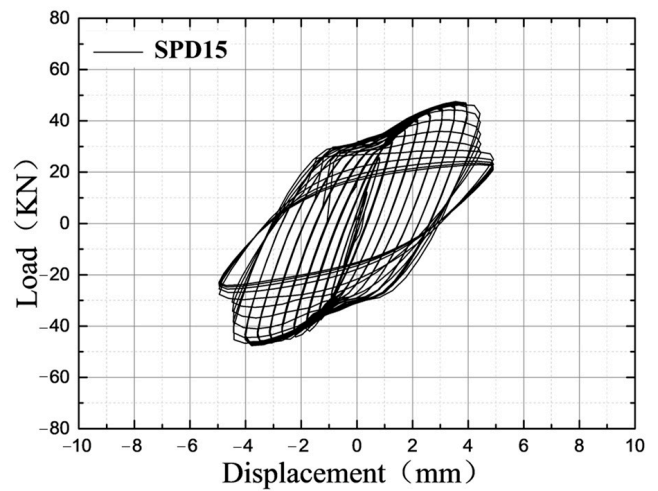(**c**) Opening Rate of 20%

(**d**) Opening Rate of 25%
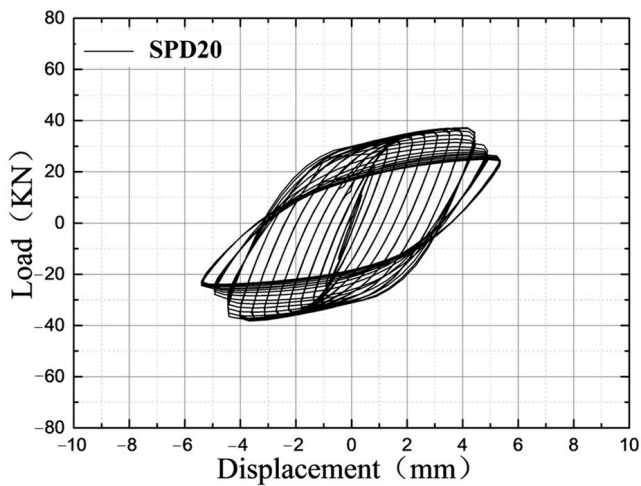
Figure 9. Hysteresis curve of SPC damper.

Figure 10 is the hysteresis curve of the SPD series shear plate damper. It can be seen from the diagram that the form and change trend of the SPD hysteresis curve is between the SPA and SPB. When the opening ratio is 15%, the hysteresis curve form of the SPD damper is similar to that of the SPA series. With the increase in the opening ratio, the hysteresis curve form gradually converges to the SPB series. After the failure of the structure, the bearing capacity is maintained at about 20 KN, and the difference in the bearing capacity of the dampers with four opening ratios is not obvious. From the point of view of the failure form, the crack generally starts from the upper and lower edges of one side of the column hole, and the strip begins to damage from the edge of the shear plate. After the failure, the adjacent strips begin to damage, and finally, all the strips on one side are damaged.
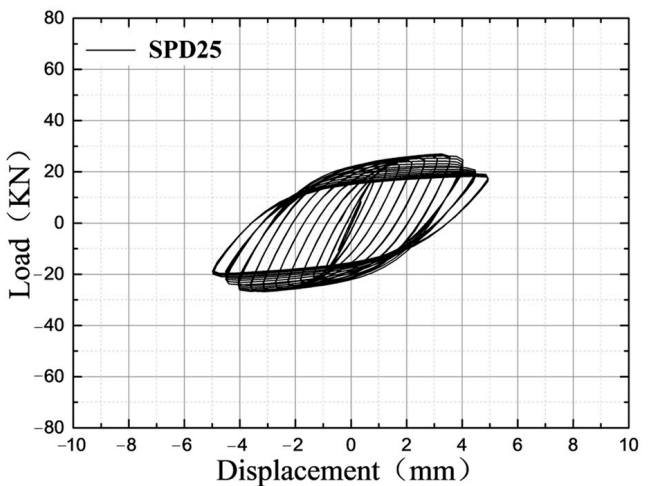
(**a**) Opening Rate of 10%

(**b**) Opening Rate of 15%

(**c**) Opening Rate of 20%

(**d**) Opening Rate of 25%

Figure 10. Hysteresis curve of SPD damper.

The skeleton curves of the shear plate dampers with different opening forms are shown in Figure 11. The skeleton curves are typical two-fold lines, and the skeleton curves before yielding are similar to straight lines. The ductility coefficient is generally the ratio of the ultimate displacement to the yield displacement (because the length of each shear plate damper is the same, the ductility coefficient is the ratio of the ultimate shear angle to the yield shear angle). Combined with the hysteresis curves of each shear plate damper, it can be seen that SPA10 yielded the earliest, and its yield shear angle was only 22% of the yield shear angle of SPB15, but its ductility was better. However, it should be pointed out that the reason for the large ductility coefficient is that the yield shear angle is very small. Measured by the ultimate shear angle, although the ultimate shear angle is larger than the other shear plate dampers (except SPC25), once its deformation exceeds the ultimate shear angle, the bearing capacity decreases rapidly, and the peak shear angle is not much different from the ultimate shear angle. On the whole, the SPA series has the highest bearing capacity, the largest peak shear angle, the largest ultimate shear angle, and the highest ductility coefficient.
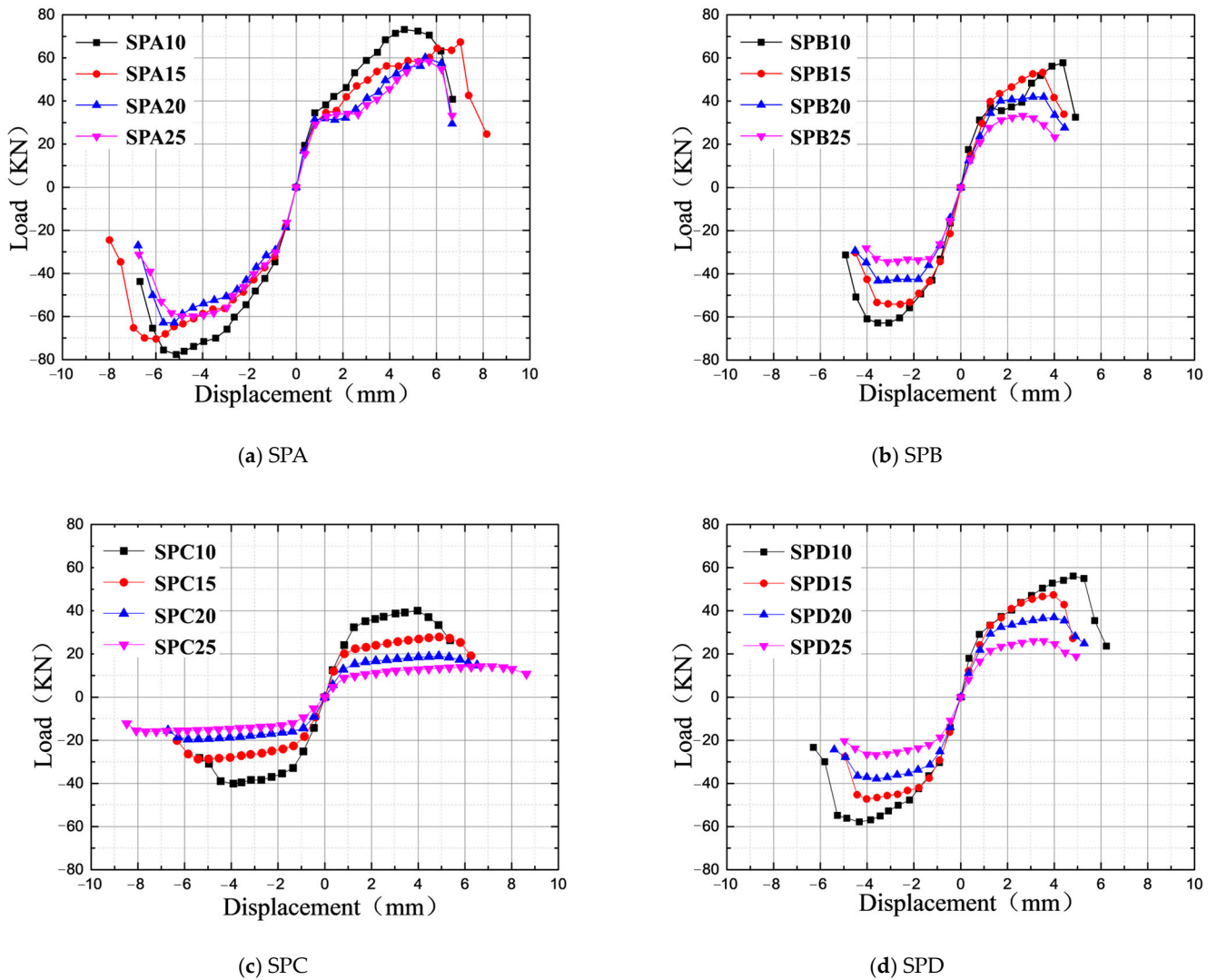
(**a**) SPA

(**b**) SPB

(**c**) SPC

(**d**) SPD

Figure 11. Skeleton curves of dampers with different opening forms.

3.3. Cyclic Hysteretic Energy Dissipation

The energy dissipation capacity is an index to measure the anti-vibration performance of the shear plate damper, which reflects the ability of the damper to dissipate energy under reciprocating loading. Taking the hysteresis loop area, $\sum E_t$, as the energy consumption index, the summary results are shown in Table 3. Among them, $\sum E_t$ is the area of the hysteresis curve, which represents the hysteretic energy dissipation capacity of the damper. $\sum E$ represents the energy dissipation capacity of the unit volume damper, which is calculated as shown in Formula (1), where φ is the opening ratio of the damper. Figure 12 lists the hysteretic energy dissipation curves of four types of dampers.

$$\sum E = \frac{\sum E_t}{1 - \varphi} \tag{1}$$

In Figure 12 and Table 3, it can be seen that under the same loading amplitude, the smaller the opening rate, the greater the hysteretic energy consumption. Among them, the SPD series 10% and 15% opening rate dampers have similar energy consumption before the 5 mm loading step. SPA15 has the largest energy consumption value in the SPA series, and the 10% opening rate form of SPB and SPD series has the largest energy consumption value. Due to the small stiffness of the SPC series, the larger the opening ratio, the better the ductility, the longer the hysteresis time, and the stronger the energy dissipation capacity.

The results show that the energy dissipation performance of SPA series shear plate dampers is better than that of other series dampers.

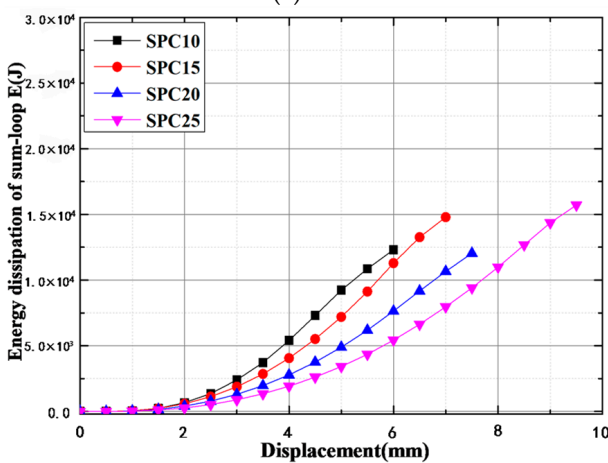**Table 3.** Energy dissipation performance of different series of shear plate dampers.

Type	$\sum E_t$ (kN·m)	$\sum E$ (kN·m)
SPA10	25.48	28.31
SPA15	24.11	28.36
SPA20	20.28	25.35
SPA25	15.01	20.01
SPB10	21.85	24.28
SPB15	16.62	19.56
SPB20	17.71	22.14
SPB25	13.25	17.67
SPC10	17.77	19.74
SPC15	15.93	18.75
SPC20	14.51	18.14
SPC25	12.42	16.56
SPD10	17.65	19.61
SPD15	15.90	18.71
SPD20	16.74	20.93
SPD25	15.40	20.53
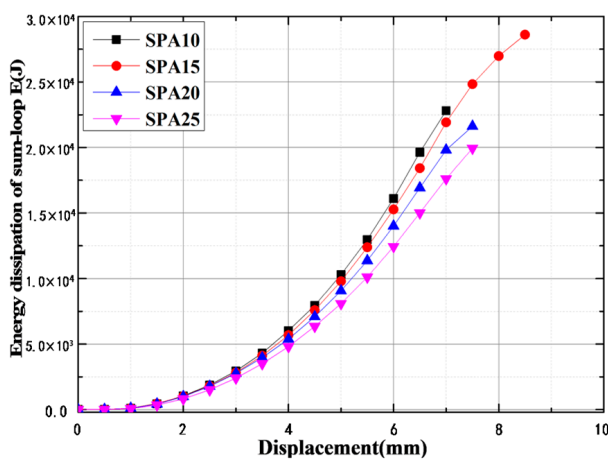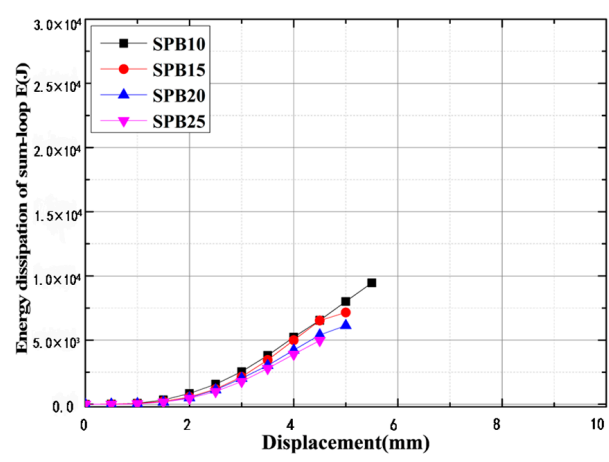
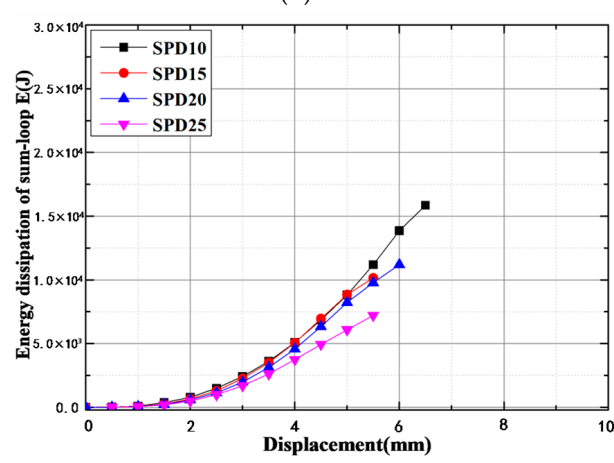**Figure 12.** Energy dissipation performance of dampers with different opening forms.

4. Conclusions and Future

In this paper, the energy dissipation performance of a new type of shear plate metal damper with upper and lower elliptical openings is systematically studied. The hysteretic curve, skeleton curve, and cyclic hysteretic energy dissipation capacity are analyzed by loading tests. The relevant conclusions are as follows:

(1) When the opening ratio is 25%, SPA, SPB, and SPD have a certain overall out-of-plane phenomenon, while SPC has a local out-of-plane phenomenon due to the small central stiffness, but the overall planeness is better.

(2) The bearing capacity of the SPA series is the highest, and the peak shear force reaches 74.22 KN, which is 19–46% higher than that of the other three dampers (the opening rate is 10%).

(3) The bearing capacity and energy dissipation performance of the SPA series shear plate dampers are better than other series dampers, and the energy dissipation capacity is 44–48% higher than the other three dampers (the opening rate is 15%).

In summary, the energy dissipation performance of the SPA series shear plate dampers is better than that of other series dampers, which can solve the problem of excessive vertical vibration of the jacket platform under the action of the seismic primary wave. Through experimental phenomena and theoretical analysis, it can be seen that the SPA series shear plate damper has reasonable force and better performance than other forms of shear plate structure. Moreover, the structure is simple and easy to replace after an earthquake, which has a good application prospect in the seismic field of jacket platforms.

In the future, the author will compare the performance of the new type of shear plate damper with upper and lower elliptical openings proposed in this paper with other available dampers on the market to further verify the performance of the new damper.

References

1. International Renewable Energy Agency. *Renewable Capacity Statistics 2022*; The International Renewable Energy Agency: Masdar City, United Arab Emirates, 2022.
2. World Bank Group. Commodity Markets Outlook. Washington DC, World Bank, 2022. Available online: https://www.worldbank.org/en/research/commodity-markets (accessed on 11 May 2023).
3. Graff, W.J. *Introduction to Offshore Structures: Design, Fabrication, Installation*; Gulf Publishing Company: Houston, TX, USA, 1981.
4. Wang, L.; Zhou, W.; Guo, Z.; Rui, S. Frequency Change and Accumulated Inclination of Offshore Wind Turbine Jacket Structure with Piles in Sand Under Cyclic Loadings. *Ocean. Eng.* **2020**, *217*, 108045. [CrossRef]
5. Ma, Z.; Lou, Z.; Zhai, G.; Li, J. Surge Response Analysis of the Serbuoys-TLP Tension Leg Platform under the Action of Wave-Current Coupling. *J. Mar. Sci. Eng.* **2022**, *10*, 571. [CrossRef]
6. Ma, Z.; Li, J.; Li, B. Research on the Grid Connected Stability of Wind Turbine-Energy Storage Combined Power Systems Based on a New Wind Power Fluctuation Smoothing Strategy. In Proceedings of the 2023 3rd International Conference on Energy Engineering and Power Systems (EEPS), Dali, China, 28–30 July 2023.
7. Sun, J. Dynamic Response Analysis of a Jacket Platform under Strong Earthquake Based on an Endurance Time Method. *J. Vib. Control* **2020**, *39*, 232–241.
8. Mo, R.; Cao, R.; Liu, M.; Li, M. Effect of Ground Motion Directionality on Seismic Dynamic Responses of Monopile Offshore Wind Turbines. *Renew. Energ.* **2021**, *175*, 179–199. [CrossRef]
9. Liang, F.; Yuan, Z.; Liang, X.; Zhang, H. Seismic Response of Monopile-Supported Offshore Wind Turbines under Combined Wind, Wave and Hydrodynamic Loads at Scoured Sites. *Comput. Geotech.* **2022**, *144*, 104640. [CrossRef]

10. Zhang, B.; Han, Q.; Zhang, X.; Yu, X. Sliding Mode Control with Mixed Current and Delayed States for Offshore Steel Jacket Platforms. *IEEE T Contr Syst. T* **2014**, *22*, 1769–1783. [CrossRef]

11. Tian, X.; Wang, Q.; Liu, G.; Liu, Y.; Xie, Y.; Deng, W. Topology Optimization Design for Offshore Platform Jacket Structure. *Appl. Ocean. Res.* **2019**, *84*, 38–50. [CrossRef]

12. Zheng, Z.; Chang, Z.; Zhao, L. Mitigating Deepwater Jacket Offshore Platform Vibration under Wave and Earthquake Loadings Utilizing Nonlinear Energy Sinks. *Ocean. Eng.* **2023**, *283*, 115096. [CrossRef]

13. Ou, J.; Long, X.; Li, Q.S.; Xiao, Y.Q. Vibration Control of Steel Jacket Offshore Platform Structures with Damping Isolation Systems. *Eng. Struct.* **2007**, *29*, 1525–1538. [CrossRef]

14. Lavassani, S.H.; Gavgani, S.A.; Doroudi, R. Optimal Control of Jacket Platforms Vibrations under the Simultaneous Effect of Waves and Earthquakes Considering Fluid-Structure Interaction. *Ocean. Eng.* **2023**, *280*, 114593. [CrossRef]

15. Ding, H.; Wang, W.; Liu, J.F.; Wang, J.T.; Le, Z.J.; Zhang, J.; Yu, G.M. On the Size Effects of Toroidal Tuned Liquid Column Dampers for Mitigating Wind- and Wave-Induced Vibrations of Monopile Wind Turbines. *Ocean. Eng.* **2023**, *273*, 113988. [CrossRef]

16. Ke, K.; Yam, M.C.H.; Zhang, P.; Shi, Y.; Li, Y.; Liu, S. Self-Centring Damper with Multi-Energy-Dissipation Mechanisms: Insights and Structural Seismic Demand Perspective. *J. Constr. Steel Res.* **2023**, *204*, 107837. [CrossRef]

17. Zuo, H.; Bi, K.; Hao, H. Using Multiple Tuned Mass Dampers to Control Offshore Wind Turbine Vibrations under Multiple Hazards. *Eng. Struct.* **2017**, *141*, 303–315. [CrossRef]

18. Wang, M.; Zhang, W.Q.; Wang, P.G.; Du, X.L. Multiple Hazards Vibration Control of Jacket Offshore Wind Turbines Equipped with Amplifying Damping Transfer Systems: Winds, Waves, and Earthquakes. *Ocean. Eng.* **2023**, *285*, 115355. [CrossRef]

19. Zhang, T.; Wang, W.; Li, X.; Wang, B. Vibration Mitigation in Offshore Wind Turbine under Combined Wind-Wave-Earthquake Loads Using the Tuned Mass Damper Inerter. *Renew. Energ.* **2023**, *216*, 119050. [CrossRef]

20. Roeder, C.W.; Schneider, S.P.; Carpenter, J.E. Seismic Behavior of Moment-Resisting Steel Frames: Analytical Study. *J. Struct. Eng.* **1993**, *6*, 1866–1884. [CrossRef]

21. Kazantzi, A.K.; Righiniotis, T.D.; Chryssanthopoulos, M.K. Fragility and Hazard Analysis of a Welded Steel Moment Resisting Frame. *J. Earthq. Eng.* **2008**, *4*, 596–615. [CrossRef]

22. Zhu, Y.; Wang, W.; Lu, Y.; Yao, Z. Finite Element Modeling and Design Recommendations for Low-Yield-Point Steel Shear Panel Dampers. *J. Build. Eng.* **2023**, *72*, 106634. [CrossRef]

23. Enferadi, M.H.; Ghasemi, M.R.; Shabakhty, N. Wave-Induced Vibration Control of Offshore Jacket Platforms through SMA Dampers. *Appl. Ocean. Res.* **2019**, *90*, 101848. [CrossRef]